Available online at www.sciencedirect.com
SCIENCE DIRECT
ELSEVIER
International Journal of Mass Spectrometry 249–250 (2006) 155–161
International Journal of Mass Spectrometry
www.elsevier.com/locate/ijms

# Direct determination of the ionization energy of histidine with VUV synchrotron radiation

Kevin R. Wilson [a], Leonid Belau [a], Christophe Nicolas [a], Michael Jimenez-Cruz [a], Stephen R. Leone [a,b], Musahid Ahmed [a,*]

[a] *Lawrence Berkeley National Laboratory, Chemical Sciences Division, University of California, Berkeley, CA 94720, United States*
[b] *Departments of Chemistry and Physics, University of California, Berkeley, CA 94720, United States*

Received 3 October 2005; received in revised form 22 December 2005; accepted 27 December 2005
Available online 7 February 2006

**Abstract**

Intact molecules of histidine are generated in the gas phase using impaction of nanoparticles on a heater. The direct determination of the ionization energy (IE) of histidine (155 *m*/*z*) is performed using single photon ionization with tunable vacuum ultraviolet (VUV) synchrotron radiation and is reported to be 8.2(±0.1) eV. Ab initio calculations are performed at the B3LYP/6-311G (UB3LYP/6-311G) level of theory generating vertical and adiabatic ionization energies and possible fragmentation mechanisms. The theoretical adiabatic ionization energies derived for two lying conformers of histidine agree very well with the experimental result. Thermal dissociation at the heater gives rise to fragments, which are subsequently photoionized generating *m*/*z* 82 and 111, while *m*/*z* 110 is formed by dissociative photoionization of the histidine cation. Appearance energies of fragment ions at *m*/*z* 82, 110 and 111 are 8.5(±0.1), 8.5(±0.1) and 8.4(±0.1) eV, respectively, at a heater temperature of 373 K. The H-atom dissociation energy of protonated histidine is derived to be 4.8(±0.1) eV using thermodynamic arguments.
Published by Elsevier B.V.

*Keywords:* Ionization energies; Amino acids; Single photon ionization; Biological nanoparticles; Ab-initio calculations

## 1. Introduction

Amino acids and nucleic bases are two of the most important building blocks of life. Gas phase studies on these molecules are essential to extract thermochemical information as these are key to understanding fragmentation patterns [1] in proteomic [2] and genomic [3] sequencing experiments. Small peptide ions in the gas phase, the components of which are individual amino acids, have been recognized as interesting candidates to study intramolecular electron transfer free from any solvent effects [4]. To gain an understanding of the dynamics of these processes, ionization energies of the individual amino acids are required.

Traditional gas phase photodissociation methods are increasingly being used to understand fragmentation patterns and the nature of excited states in amino acids [5]. Recently, ultrafast photo-induced fragmentation studies have been performed on protonated amino acids to elucidate excited state dynamics in the gas phase [6]. The drive to generate new types of bio-devices has led to studies on the arrangement of amino acids on semiconductor surfaces [7]. A crucial component in all these studies is the ionization energies of amino acids in isolated gas phase environment; such values can be confirmed by electronic structure calculations. It is imperative that reliable experimental values are available for comparison with theory.

Determinations of ionization energies and other properties of amino acids in the gas phase are not trivial. The challenge stems from the fact that transporting these non-volatile and in most cases very fragile molecules to the gas phase leads to extensive fragmentation, making it difficult to generate intact parent molecules. Ingenious techniques have been developed to transport these molecules successfully into the gas phase [8]. It is now routine using soft ionization techniques, such as MALDI and electrospray ionisation, to generate these species, albeit in the protonated form. Laser and thermal desorption techniques in conjunction with jet cooling, pioneered most notably by the groups of Levy and co-workers [9], de Vries and co-workers [10] and Grotemeyer and Schlag [11], have led to an explosion of measurements of the photoionization dynamics

* Corresponding author. Tel.: +1 510 486 6355; fax: +1 510 486 5311.
*E-mail address:* mahmed@lbl.gov (M. Ahmed).

1387-3806/$ – see front matter. Published by Elsevier B.V.
doi:10.1016/j.ijms.2005.12.044

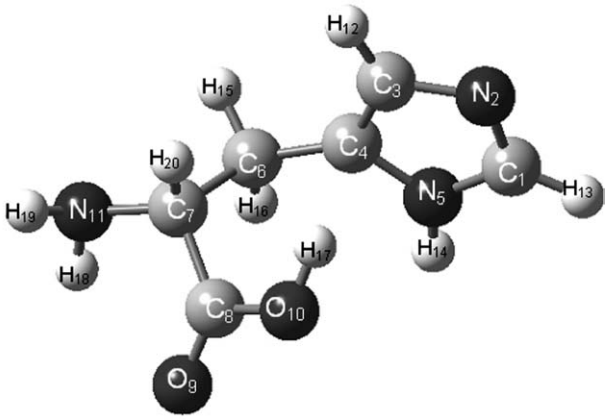


Fig. 1. Molecular structure of histidine and numeration of atoms therein.

and electronic spectroscopy of neutral amino acids and small peptides.

There have been a number of photoelectron spectroscopy (PES) determinations of the ionization energies of amino acids in the past [12–15]. However, the ionization energies of 7 of the 20 naturally occurring amino acids are still unknown. Very recently, there has been a resurgence of experiments aimed at studying the photoionization dynamics of amino acids. These efforts are being pursued in part to understand conformational structures of these amino acids. Powis et al. [16] performed a very elegant study on alanine and threonine using synchrotron radiation photoelectron spectroscopy, while Lee et al. [17] measured the ionization energies of different conformers of phenylalanine using resonant two photon ionization spectroscopy. Direct photoionization mass spectrometry for a number of amino acids with synchrotron radiation was reported recently and ionization energies were determined for glycine, alanine and amino-isobutyric acid [18].

Beauchamp's [14] group has performed extensive correlation studies of adiabatic ionization energies with proton affinities to derive qualitative and mechanistic information for the amino acids and related compounds. Histidine (Fig. 1) and arginine are notably absent since their ionization energies are unknown. They conjecture that there should be substantial deviations from the correlation trend for these two amino acids, which are strongly basic in nature, since they can be protonated preferentially on the side-chain instead of the amino group. Dimer formation could also play a role since these amino acids can cyclize in acidic media and lose water. Histidine plays a very important role in biological function due to the proton acceptor capability of the imidazole ring through its two side-chain nitrogen atoms.

There has been a large body of theoretical work characterizing the electronic properties of amino acids [19]. This is driven partly by the quest to understand crystal structure and to probe the existence of zwitterions of amino acids in the gas phase. However, electronic structure calculations on neutral histidine and its cation in the gas phase are rare; to our knowledge there has been only one study [20]. In that work, relative energies and adiabatic ionization energies of four different histidine configurations were calculated using the B3LYP formalism.

Here, we report the direct determination of the ionization energy of histidine using tunable vacuum ultraviolet (VUV) synchrotron radiation coupled to a novel bio-nanoparticle mass spectrometer. The measured ionization energy is compared to ab-initio calculations performed by us. Appearance energies of daughter ions are also reported. In addition, the H-atom dissociation energy of protonated histidine is derived using thermodynamic arguments.

## 2. Experimental

The apparatus and technique used to generate fragment free mass spectra of fragile biomolecules incorporates an aerosol particle mass spectrometer coupled to a VUV synchrotron radiation source [21]. Polydisperse nanoparticles are generated by atomizing solutions of histidine (1 g/L of $H_2O$). The solvent is evaporated using a heater and diffusion dryer and the dry nanoparticles are entrained in a carrier gas of nitrogen. The average particle diameter is determined with a commercial differential mobility analyzer coupled to a condensation particle counter and found to be 150 nm. A 1.5 mm focused beam of the particles is prepared by passing the flow of gas and particles through a set of aerodynamic lenses. After exiting a skimmer, the particles are impacted on a copper heater, which is located between the time-of-flight optics of a VUV mass spectrometer. The temperature range of the heater for this particular experiment was varied between 373 and 573 K. The gas phase biomolecules produced by particle vaporization are ionized with tunable VUV light produced by the Advanced Light Source at the Chemical Dynamics Beamline located at Lawrence Berkeley National Laboratory. This undulator-based beamline produces tunable (7.2–25.4 eV) VUV radiation at an average photon flux of $1 \times 10^{16}$ photon/s with a resolution of ~0.2 eV. However, this does not limit the resolution of the ionization onset determinations, as will be described in Section 4. The synchrotron light is passed through an argon gas filter and two $MgF_2$ windows to remove high energy harmonics produced by the undulator. The photon beam spot size is ~200 μm in the region where the photon and particle beam intersect. One stage of differential pumping is used to couple the time-of-flight (TOF) spectrometer to the ultrahigh vacuum (UHV) environment of the beamline ($10^{-7}$ Pa). A home made dual-stage pulsed acceleration TOF is used to transfer the ions across a field free tube, where the ions are subsequently detected on a microchannel plate (MCP) detector. The resulting signal is passed through a preamplifier and the signal is collected with a multiscaler (FAST Comtec P7886). The undulator is continuously scanned and TOF mass spectra are collected in 0.1 eV steps. After correction for photon flux and energy calibration, photoionization efficiency curves are extracted for each mass.

## 3. Computational method

The atom labeling of histidine ($C_6H_9N_3O_2$) is shown in Fig. 1. It has 54 vibrational degrees of freedom. Our principal aim here is not to fully describe the potential energy surface (PES) of histidine ground state (GS), but to optimize and estimate adiabatic and vertical ionization energies for a few

low-lying stable conformers and to compare them to our experimental value. Using energetic arguments, we chose only 7 lowest-lying conformers from 36 calculated geometries that could be populated upon thermal excitation. Miscellaneous assemblies of starting geometries differ mainly in the four dihedral angles: D1($C_8$–$C_7$–$C_6$–$C_4$), different configurations of imidazole ring and carboxyl moiety; D2($C_7$–$C_6$–$C_4$–$C_3$), rotations of imidazole ring around $C_6$–$C_4$ bond; D3($N_{11}$–$C_7$–$C_8$–$O_9$) and D4($C_7$–$C_8$–$O_9$–$H_{20}$), cis and trans conformations of the amino and carboxyl hydrogens, respectively.

The geometries of a number of predicted conformers have been fully optimized at the B3LYP/6-311G theoretical level followed by vibrational analysis in order to confirm the nature of the critical point on the PES.

The vertical ionization energy ($IE_v$) of each conformer has been calculated by freezing the optimized geometries of the GS and removing one electron from the highest occupied molecular orbital (HOMO) according to Koopman's theorem. $IE_v$ is defined as

$$IE_v = E(GS) - E^+(GS)$$

where $E$(GS) and $E^+$(GS) are the total electronic energy of the neutral and ionized conformer, respectively, in the optimized ground state conformation. In an attempt to calculate the GS energies of the ionized conformers, the full optimization of the GS geometry of the corresponding neutral conformer has been improved, utilizing the electronic configuration of the open shell ionized molecule. Each conformer geometry optimization is followed by vibrational analysis in order to predict the topological nature of the optimized geometry on the PES of the ion state and to introduce the zero point vibrational energy (ZPE) correction to the total energy. The local adiabatic ionization energy ($IE_a$) of the conformers is calculated according to the following equation:

$$IE_a = E(GS) + ZPE(GS) - E^+(CGS) - ZPE^+(CGS)$$

where $E^+$(CGS) is the total electronic energy of a fully optimized cationic ground state conformer, and ZPE(GS) and $ZPE^+$(CGS) correspond to the correction values for ground state of the neutral and ionized molecule, respectively.

The energies and geometry optimization of ionized conformers (open shell configurations) have been calculated at the same theoretical level utilizing the unrestricted B3LYP/6-311G (UB3LYP/6-311G) method. Calculations were performed on a Pentium (IV) CPU computer (3 GHz), utilizing the Gaussian 98W program package [22].

## 4. Results and discussion

### *4.1. Time-of-flight mass spectra and fragmentation mechanisms*

Fig. 2 shows a TOF mass spectrum obtained by photoionizing histidine at 8.6 eV with the heater temperature set at 373 K. The major peak is a fragment ion at $m/z$ 82, followed by the parent at $m/z$ 155. Two small peaks at $m/z$ 110 and 111 are also observed. Two of the fragments ($m/z$ 82 and 111) appear to form

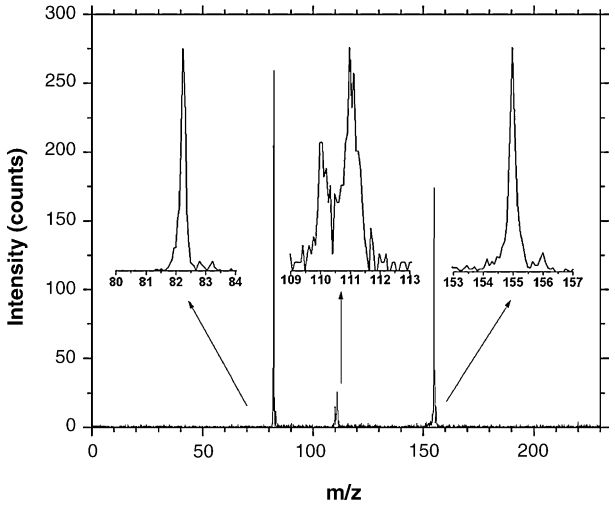


Fig. 2. Time-of-flight mass spectrum of histidine. The heater temperature is 373 K and incident photon energy is 8.6 eV. The three insets show expanded mass spectra between the ranges of $m/z$ 80–84, 109–113, 153–157.

by thermal dissociation at the heater followed by photoionization. We will discuss the nature of the fragmentation processes which gives rise to these daughter ions below. To date there has been only one mention in the literature of the detection of intact histidine in the gas phase in mass spectrometry [23]. Grotemeyer et al. vaporized L-histidine hydrochloride using $CO_2$ laser radiation and subsequently jet-cooled the resulting histidine in a molecular beam. Multiphoton resonant and non-resonant photoionization with tunable UV lasers gave rise to the detection of intact histidine ($m/z$ 155) and daughter ions at masses 81 and 110. Masses 81 and 110 will result from direct cleavage of the $C_6$–$C_7$ bond (Fig. 1) and elimination of COOH, respectively. Extensive bond cleavage has been observed in the case of another aromatic amino acid, tryptophan, with an increase in this fragmentation pathway with both incident photon energy or heater temperature [21]. The absence of mass 81 in our histidine TOF would suggest that the multiphoton fragmentation processes observed by Grotemeyer et al. [23] are different from single photon threshold ionization. Apart from this multiphoton ionization work and the observations here, to our knowledge, there is no other reported mass spectrum of neutral histidine.

There is a large body of work in which the thermal decomposition of amino acids has been characterized with analytical techniques [24–26]. However, for histidine [27], the results are inconclusive and we cannot compare our nanoparticle thermal impact studies to these experiments. There is a plethora of techniques dealing with the generation and subsequent fragmentation of protonated histidine [28–33]. While direct comparison of fragmentation channels from these studies with the neutral case is not necessarily valid, the fragmentation behavior in these systems could act as a guide to the identity of the daughter ions. The mass $m/z$ 82, which has been identified as methyl imidazole in previous collision-induced dissociation (CID) studies [31], was detected and a reaction mechanism postulated by El Aribi et al. [33] on protonated histidine.

The photoionization efficiency (PIE) curves for histidine and the daughter ions detected at $m/z$ 82, 110 and 111 with the

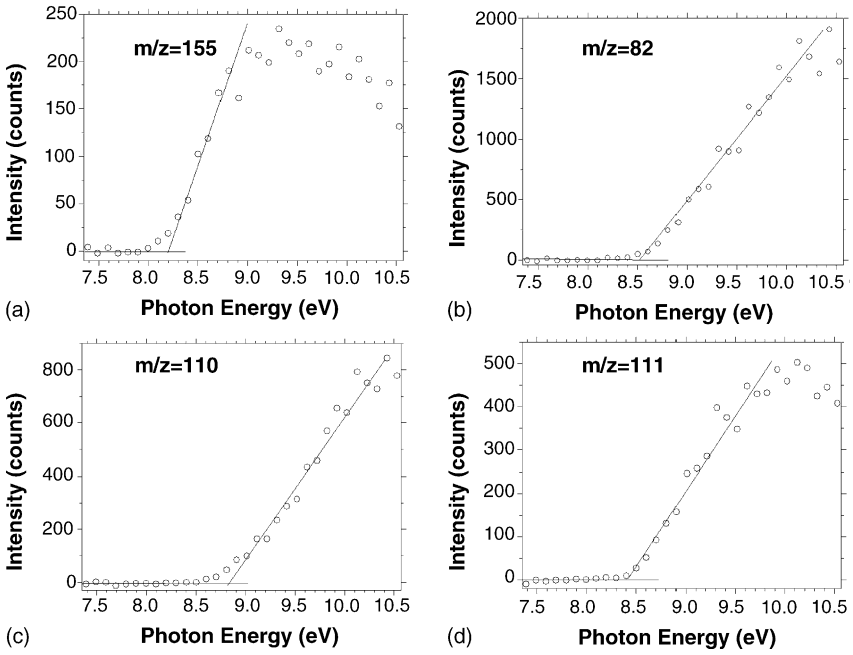


Fig. 3. Photoionization efficiency curves at 373 K for (a) histidine (*m*/*z* 155), (b) *m*/*z* 82, (c) *m*/*z* 110 and (d) *m*/*z* 111. Also shown are the non-linear least squares fits to the straight part of the slopes.

heater temperature at 373 K are shown in Fig. 3a–d, respectively. Using a non-linear least squares fitting technique, we derive appearance energies (AE) of $8.5 \pm 0.1$ and $8.4 \pm 0.1$ eV for *m*/*z* 82 and 111, respectively, at a heater temperature of 373 K. The errors quoted in these measurements are derived from the least squares fit uncertainties. In the case of *m*/*z* 110, the AE is derived from the first detection of ion signal over the baseline and is $8.5 \pm 0.1$ eV. We tentatively assign *m*/*z* 82 as 4-methyl-1H-imidazole. The vertical ionization energy of 1-methyl-1H-imidazole and 2-methyl-1H-imidazole have been measured to be 8.66 and 8.50 eV, respectively, with photoelectron spectroscopy [34]. As a first approximation, the appearance value of 8.5 eV for *m*/*z* 82 suggests that it is indeed methyl imidazole that is being detected and 8.5 eV is the ionization energy for that particular fragment. It is also important to note that there is a relatively sharp rise for the onset of this mass in contrast to other fragmentation products that have been observed by us in the case of VUV photoionization of a number of organic acids (oleic, linoleic, linolenic) and cholesterol [35]. In that work, other fragment ions show a gradual onset, which increases sharply after a certain threshold is reached. In those cases, the dissociation onsets for the primary fragment ions lie very close to the parent IE, suggesting that the parent ions are not very stable. In other words, dissociative ionization of the histidine parent would give rise to these fragment ions. This kind of behavior is observed in the case of *m*/*z* 110 (Fig. 3c), where the ionization onset is at 8.5 eV, followed by a gradual increase in ion signal. A least squares fit to the slope crosses the baseline at around 8.8 eV. In the case of *m*/*z* 82 from neutral histidine, we suggest that this species is being formed prior to ionization by neutral dissociation of the parent at the heater tip. This would explain the large enhancement and almost linear ion signal increase as function of photon energy, when the ionization onset threshold is reached. It is possible that dissociative ionization might also be at play at higher photon energies, as seen in the case of tryptophan [21], however this will be obscured by the relatively large neutral dissociation channel. Increasing the heater temperature (not shown) leads to a huge enhancement of all the fragment ions at low photon energies, particularly *m*/*z* 82, suggesting that neutral dissociation of the parent histidine is indeed enhanced. The similarity of the PIE curve for *m*/*z* 111 (Fig. 3d) to that of *m*/*z* 82 would also suggest that this species is formed by neutral dissociation at the heater followed by photoionization.

Fig. 4 summarizes what we believe are the mechanisms that give rise to the four masses that are observed in our experiment. Apart from the histidine cation at *m*/*z* 155, which is formed by direct ionization of the neutral, the fragment at *m*/*z* 110 could be formed by elimination of the carboxyl radical from the histidine cation. The radical site on the nitrogen atom, formed in photoionization, donates an electron and forms a double bond between the nitrogen and carbon atoms ($N_{11}$ and $C_7$). The second electron is donated from the carbon–carboxyl bond leading to the formation of the COOH radical.

The species at *m*/*z* 111 can be formed in the neutral channel by rearrangement of a proton from the COOH moiety to the imidazole ring with concomitant elimination of $CO_2$. It is well known that decarboxylation of amino acids takes place under pyrolysis conditions [24]. As shown in Fig. 4, we suspect this is a thermal elimination process taking place in the vicinity of the heater. Finally, *m*/*z* 82 most probably comes from a one to three proton transfer and subsequent elimination of neutral daughter fragments since we do not see the co-fragment *m*/*z* 73 under any of our conditions. It is possible the *m*/*z* 73 falls apart concomitantly to give rise to CO, HCN and $H_2O$, species whose IE's are higher than 11.0 eV. Unfortunately, we could not access photon energies higher than 11.0 eV due to the transmission limit

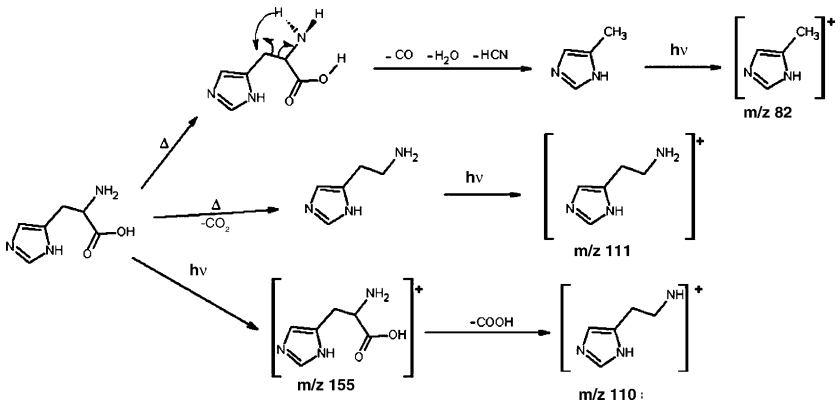


Fig. 4. Fragmentation and photoionization pathways for histidine. $\Delta$ and $h\nu$ represent thermal energy from the copper heater and single photon ionization, respectively.

of the $MgF_2$ window used to filter out the higher harmonics in the experiment and hence cannot confirm these mechanisms. Removing the $MgF_2$ window gave unusable results due to fragmentation from other photoionization events; definitive results will require access to the monochromatized VUV beamline in the future.

### 4.2. Ionization energy of histidine

Fig. 3a shows the photoionization efficiency (PIE) curve for histidine ($m/z$ 155) at a heater temperature of 373 K. A least squares fit to the slope intercepts the origin at 8.2 eV. As this slope at the onset is relatively sharp it would suggest that we are accessing the adiabatic ionization threshold for histidine, rather than a shifted, higher energy vertical ionization onset and we assign the IE at $8.2 \pm 0.1$ eV. Two factors contribute to the uncertainty in the ionization energy determination. As has been shown by our ab-initio calculations (Fig. 5), described below, several low-lying conformers can exist in the gas phase. We calculate the average internal energy deposited into histidine at a heater temperature of 373 K to be 0.2 eV using RRKM theory utilizing MassKinetics [36] software. The vibrational frequencies required for this calculation were computed with Gaussian 98 [22]. This would suggest that as many as five conformers may be populated leading to a smearing out of the ionization energy onset. Secondly, Frank–Condon factors could play a role in defining ion intensities due to substantial geometry changes that could result while moving from the neutral to the cation. Finally, these experiments are performed using broad band undulator radiation, which under our conditions generates light with a bandwidth of 0.2 eV FWHM. However, as demonstrated recently [35], PIE curves of three reference gases with known ionization energies ($C_6H_5Cl$, $C_6H_5Br$ and $C_6H_5I$) can be used to calibrate the photon energy and to obtain ionization energies with a precision of $\pm 0.06$ eV, that is better than the 0.2 eV photon band pass. This suggests that the uncertainty in the ionization energy measurement is not limited by photon resolution but is due to the two factors mentioned above. Increasing the heater temperature did not change the shape of the PIE curve for parent histidine; hence the ionization energy determination is independent of temperature. This is very similar to that observed in tryptophan using the same technique [21].

Fig. 5 shows the optimized geometric structures of some low-lying conformers of histidine and the respective cations following single photon ionization. The first three conformers lie within 0.02 eV of each other, while a cluster of four other conformers are approximately 0.2 eV above the global minimum. The local vertical and adiabatic ionization energies are graphically tabulated in Fig. 5. An examination of these conformers and energies shows that ionization from conformers 2 and 3 give rise to cations that are very similar in structure to the neutral species and furthermore give rise to local adiabatic ionization energies of 8.16 eV, in excellent agreement with the measured value of 8.2 eV. Ionization from the lowest energy conformer gives rise to a cation with a substantially different geometry when compared to the neutral conformer. The hydrogen atoms on $C_6$ point away from the imidazole ring and will probably give rise to poor Franck–Condon factors for ionization. In the PIE spectrum shown in Fig. 3a, there is evidence of histidine being ionized below 8.2 eV, the appearance energy being 8.0 eV. A candidate for this could be ionization from conformer 4 whose local adiabatic ionization energy is calculated to be 7.98 eV and gives rise to a cation with very little geometry change. As mentioned in the previous paragraph, a heater temperature of 373 K will deposit about 0.2 eV internal energy into histidine and thereby populate conformer 4, which is 0.19 eV above the ground state. This population is, however, very small, otherwise there would be substantial intensity in the parent ion signal at 8.0 eV. It is also entirely possible that ionization below 8.2 eV could arise from vibrational hot bands that are populated in neutral histidine when heated at 373 K. Ionization from conformers 5 and 6 give rise to unstable cations with fragmentation along the $C_6$–$C_7$ bond (Fig. 1) producing $m/z$ 74 and 81. We do not observe these masses even at heater temperatures of 573 K. The signal-to-noise ratio of the typical observed masses is >100. It is of course entirely possible that even when these states are populated, they will decay back to lower states through collisions near the heater prior to photoionization.

Campbell et al. [14] compared the gas phase proton affinities of amino acids with adiabatic ionization energies derived from photoelectron spectra. Using primary aliphatic amines as reference species, they found a linear correlation for those amino acids that protonate on the amine group. Data for histidine was missing since the ionization energy was unknown. Using

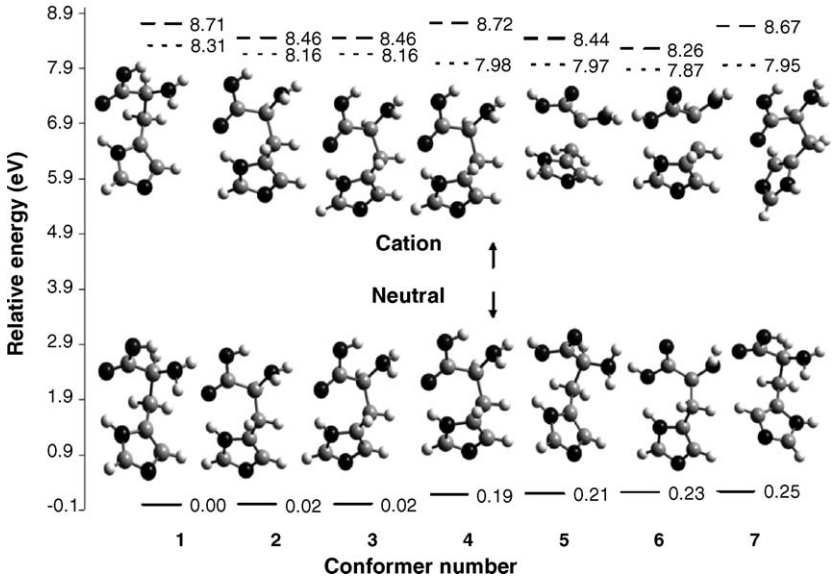


Fig. 5. Ab-initio structures of seven low-lying conformers of histidine and respective cations. Also shown are the ground state energies of neutral histidine (solid line) and the vertical (long dashed line) and adiabatic (short dashed line) ionization energies in eV.

tabulated proton affinities in conjunction with our IE value for histidine, the results show a large deviation from the correlation plotted by Campbell et al. This observed deviation, which is 0.3 eV less than the projected correlation originally postulated by these authors, could stem from stabilization of radical ions or conjugate acids of *n*-donor bases since, in the case of histidine, protonation could be favored on the side-chain instead of the amine group. In addition, intramolecular hydrogen bonding between the basic side-chain and the amine site could lead to deviations, as was noticed for lysine, methionine and tryptophan by these authors.

### *4.3. H-atom dissociation energy from protonated histidine*

The ionization energy of histidine used in conjunction with the proton affinity in a thermodynamic cycle allows for the determination of the H-atom dissociation energy ($D_H$) from protonated histidine using the following equation

$$D_H = PA_{His} + IE_{His} - IE_H$$

where $PA_{His}$, $IE_{His}$ and $IE_H$ are the proton affinity of histidine, the ionization energy of histidine and the ionization energy of the hydrogen atom, respectively. Using $IE_H = 13.6$ eV [37], $IE_{His} = 8.2$ eV from this work and $PA_{His} = 10.2$ eV from Harrison's evaluated data [1], we calculate 4.8(±0.1) eV for the bond dissociation energy. This value, used in conjunction with electronic spectroscopy of the amino acids, should provide valuable insight towards deactivation mechanisms for photo excited biological systems, as has been detailed very elegantly by Kang et al. [6] for tryptophan, tyrosine and phenylalanine. These authors observed using ultrafast pump-probe techniques the slowing down of the decay of excited states of these amino acids with increasing bond dissociation energy as they moved along the series tryptophan, tyrosine and phenylalanine. This variation of the decay dynamics was ascribed to energy differences between the dissociative $\pi\sigma^*$ state and the initially excited $\pi\pi^*$ state. The positions of these states were estimated using the H-atom bond dissociation energies calculated using the cycle mentioned above. Following these arguments, we postulate that histidine and phenylalanine will have similar UV excitation dynamics and the 266 nm (4.66 eV) photons used by these authors for excitation will not provide enough energy for intersystem crossing within the electronic excited states of histidine.

## 5. Conclusion

The ionization energy of gas phase histidine has been determined to be 8.2(±0.1) eV utilizing tunable VUV synchrotron radiation in conjunction with thermal vaporization of aerosol nanoparticles. Aided by ab initio calculations, we have discussed the mechanistic origin of this result. This method promises to provide a simple way to measure ionization energies for fragile biomolecules and other studies are being undertaken. Thermal dissociation of histidine at the heater gives rise to neutral fragments which are subsequently photoionized giving rise to *m*/*z* 82 and 111, while *m*/*z* 110 is assigned to dissociative photoionization of histidine. Appearance energies of fragment ions at *m*/*z* 82, 110 and 111 are 8.5(±0.1), 8.5(±0.1) and 8.4(±0.1) eV, respectively, at a heater temperature of 373 K. The H-atom dissociation energy from protonated histidine is derived to be 4.8 eV using thermodynamic arguments.

## Acknowledgements

This contribution is dedicated to the memory of Chava Lifshitz. M.A. acknowledges support from the Laboratory Directed Research and Development (LDRD) program at LBNL. This work was supported by the Director, Office of Energy Research, Office of Basic Energy Sciences, Chemical Sciences Division of the U.S. Department of Energy under contract No. DE-AC02-05CH11231.

## References


[1] A.G. Harrison, Mass Spectrom. Rev. 16 (1997) 201.
[2] R. Aebersold, M. Mann, Nature 422 (2003) 198.
[3] Z.J. Meng, T.A. Simmons-Willis, P.A. Limbach, Biomol. Eng. 21 (2004) 1.
[4] R. Weinkauf, E.W. Schlag, T.J. Martinez, R.D. Levine, J. Phys. Chem. A 101 (1997) 7702.
[5] F.O. Talbot, T. Tabarin, R. Antoine, M. Broyer, P. Dugourd, J. Chem. Phys. 122 (2005) 74310.
[6] H. Kang, C. Jouvet, C. Dedonder-Lardeux, S. Martrenchard, G. Gregoire, C. Desfrancois, J.P. Schermann, M. Barat, J.A. Fayeton, Phys. Chem. Chem. Phys. 7 (2005) 394.
[7] M. Oda, T. Nakayama, Appl. Surf. Sci. 244 (2005) 627.
[8] R. Weinkauf, J.P. Schermann, M.S. de Vries, K. Kleinermanns, Eur. Phys. J. D 200 (2002) 309.
[9] T.R. Rizzo, Y.D. Park, L.A. Peteanu, D.H. Levy, J. Chem. Phys. 84 (1986) 2534.
[10] E. Nir, L. Grace, B. Brauer, M.S. de Vries, J. Am. Chem. Soc. 121 (1999) 4896.
[11] J. Grotemeyer, E.W. Schlag, Angew. Chem. Int. Ed. 27 (1988) 447.
[12] P.H. Cannington, N.S. Ham, J. Electron Spec. Rel. Phenom. 15 (1979) 79.
[13] P.H. Cannington, N.S. Ham, J. Electron Spec. Rel. Phenom. 32 (1983) 139.
[14] S. Campbell, J.L. Beauchamp, M. Rempe, D.L. Lichtenberger, Int. J. Mass. Spectrom. Ion. Proc. 117 (1992) 83.
[15] T.P. Debies, J.W. Rabalais, J. Electron Spec. Rel. Phenom. 3 (1974) 315.
[16] I. Powis, E.E. Rennie, U. Hergenhahn, O. Kugeler, R. Bussy-Socrate, J. Phys. Chem. A 107 (2003) 25.
[17] K.T. Lee, J. Sung, K.J. Lee, Y.D. Park, S.K. Kim, Angew. Chem. Int. Ed. 41 (2002) 4114.
[18] H.W. Jochims, M. Schwell, J.L. Chotin, M. Clemino, F. Dulieu, H. Baumgartel, S. Leach, Chem. Phys. 298 (2004) 279.
[19] A.G. Csaszar, A. Perczel, Prog. Biophys. Mol. Bio. 71 (1999) 243.
[20] D. Dehareng, G. Dive, Int. J. Mol. Sci. 5 (2004) 301.
[21] K. R. Wilson, M. Jimenez-Cruz, C. Nicolas, L. Belau, S. R. Leone, M. Ahmed, J. Phys. Chem. A, http://dx.doi.org/10.1021/jp0543734.
[22] G.W.T.M.J. Frisch, H.B. Schlegel, G.E. Scuseria, M.A. Robb, J.R. Cheeseman, V.G. Zakrzewski, J.A. Montgomery Jr., R.E. Stratmann, J.C. Burant, S. Dapprich, J.M. Millam, A.D. Daniels, K.N. Kudin, M.C. Strain, O. Farkas, J. Tomasi, V. Barone, M. Cossi, R. Cammi, B. Mennucci, C. Pomelli, C. Adamo, S. Clifford, J. Ochterski, G.A. Petersson, P.Y. Ayala, Q. Cui, K. Morokuma, P. Salvador, J.J. Dannenberg, D.K. Malick, A.D. Rabuck, K. Raghavachari, J.B. Foresman, J. Cioslowski, J.V. Ortiz, A.G. Baboul, B.B. Stefanov, G. Liu, A. Liashenko, P. Piskorz, I. Komaromi, R. Gomperts, R.L. Martin, D.J. Fox, T. Keith, M.A. Al-Laham, C.Y. Peng, A. Nanayakkara, M. Challacombe, P.M.W. Gill, B. Johnson, W. Chen, M.W. Wong, J.L. Andres, C. Gonzalez, M. Head-Gordon, E.S. Replogle, J.A. Pople, Gaussian Inc., Pittsburgh, PA, 2001.
[23] J. Grotemeyer, K. Walter, U. Boesl, E.W. Schlag, Int. J. Mass. Spectrom. Ion Proc. 78 (1987) 69.
[24] M.A. Ratcliff, E.E. Medley, P.G. Simmonds, J. Org. Chem. 39 (1974) 1481.
[25] P.G. Simmonds, G.P. Shulman, M.A. Ratcliff, E.E. Medley, Anal. Chem. 44 (1972) 2060.
[26] G. Chiavari, G.C. Galletti, J. Anal. Appl. Pyrol. 24 (1992) 123.
[27] R.M. Smith, G.A. Solabi, W.P. Hayes, R.J. Stretton, J. Anal. Appl. Pyrol. 1 (1980) 197.
[28] C.D. Parker, D.M. Hercules, Anal. Chem. 57 (1985) 698.
[29] G.W.A. Milne, T. Axenrod, H.M. Fales, J. Am. Chem. Soc. 92 (1970) 5170.
[30] D.J. Surman, J.C. Vickerman, J. Chem. Res. (1981) 170.
[31] N.N. Dookeran, T. Yalcin, A.G. Harrison, J. Mass. Spectrom. 31 (1996) 500.
[32] F. Rogalewicz, Y. Hoppilliard, G. Ohanessian, Int. J. Mass. Spectrom. 196 (2000) 565.
[33] H. El Aribi, G. Orlova, A.C. Hopkinson, K.W.M. Siu, J. Phys. Chem. A 108 (2004) 3844.
[34] B.G. Ramsey, J. Org. Chem. 44 (1979) 2093.
[35] E.R. Mysak, K.R. Wilson, M. Jimenez-Cruz, M. Ahmed, T. Baer, Anal. Chem. 77 (2005) 5953.
[36] L. Drahos, K. Vékey, J. Mass. Spectrom. 36 (2001) 237.
[37] http://webbook.nist.gov.